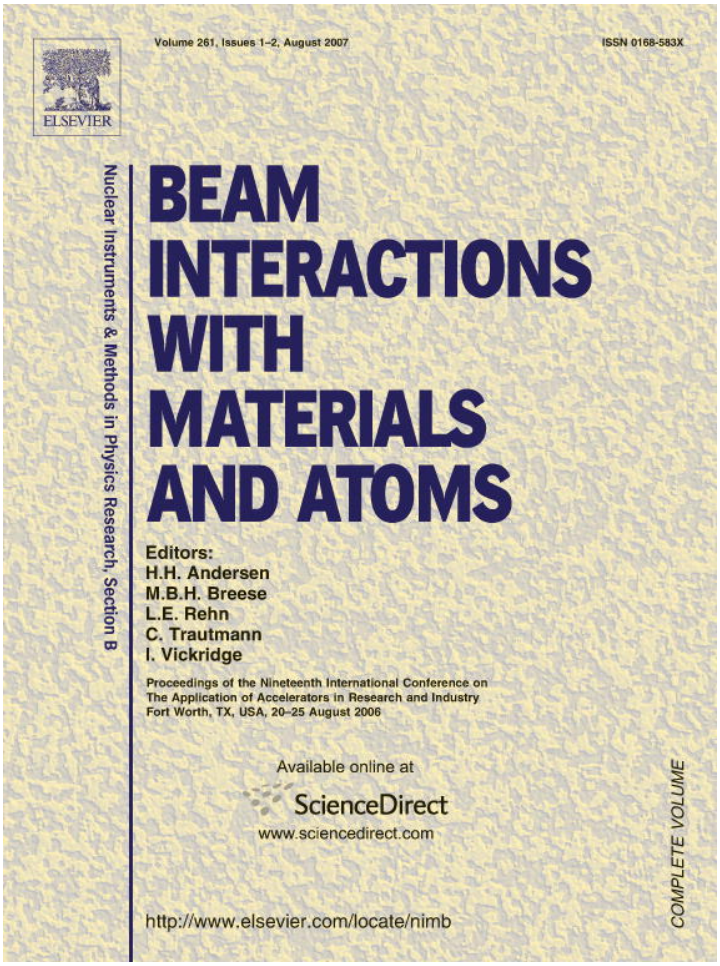

Available online at www.sciencedirect.com
ScienceDirect
Nuclear Instruments and Methods in Physics Research B 261 (2007) 175–179
NIM B
Beam Interactions with Materials & Atoms
www.elsevier.com/locate/nimb

Limitations on the validity of impulse approximation in Compton scattering

R.H. Pratt [a], L.A. LaJohn [a], T. Suric [a,b,*], B.K. Chatterjee [c], S.C. Roy [c]

[a] University of Pittsburgh, Pittsburgh, PA 15260, USA
[b] R. Boskovic Institute, 10000 Zagreb, Croatia
[c] Bose Institute, 700009 Kolkata, India

Available online 4 April 2007

Abstract

The validity of impulse approximation (IA), which is commonly used in the description of Compton scattering of photons from atomic electrons, is discussed with particular attention to the kinematical region in which the photon momentum transfer k is not much larger than the average bound electron momentum a of a given shell. IA can be justified in the Compton peak region of the spectrum if $a/k \ll 1$. However, for the doubly differential cross-section of photon–atom scattering (ejected electrons not observed) IA is commonly used, and viewed as adequate, while only requiring that $a/k < 1$. In addition to a general discussion of the validity of IA (and the relativistic version RIA) for doubly and triply differential cross-sections, in this paper, we are particularly concerned with (1) the asymmetry around the IA peak of the Compton profile and (2) the contribution of the $\vec{p}\cdot\vec{A}$ interaction term (neglected in IA) in the peak region for $a/k < 1$. We argue that the observed asymmetry of the Compton profile is to a large extent just a shift of the IA profile. We find that $\vec{p}\cdot\vec{A}$ contribution to the peak region for $a/k \approx 1$ is important only for scattering from high Z K-shells.

PACS: 32.80.Fb; 32.80.Cy

Keywords: Compton scattering; Impulse approximation; Asymmetry; Compton profile

1. Introduction

Impulse approximation (IA) is commonly used in the description of Compton scattering from atoms, the inelastic scattering of a photon in which an electron is ejected. IA involves the assumption that scattering from bound electrons can be described as scattering from a momentum distribution $\rho(\vec{p})$ of free electrons, where $\rho(\vec{p}) = |\psi(\vec{p})|^2$ and $\psi(\vec{p})$ is the Fourier transform of the coordinate space electron wave function [1–4].

In this paper, we will discuss the validity of impulse approximation, with particular attention to the kinematical region in which $a/k < 1$, where a is the average bound electron momentum and k is the photon momentum transfer. We will also discuss the contribution of the $\vec{p}\cdot\vec{A}$ interaction term (neglected in IA) in the peak region for $a/k \approx 1$.

In Section 2, we review the general treatments of Compton scattering and note new additions to our understanding. In Section 3, we discuss the difference in the validity of IA for the DDCS and the triply differential cross-section (TDCS). In Section 4, we discuss the so-called asymmetry of Compton profile and give a new definition of asymmetry. In Section 5, we discuss the importance of $\vec{p}\cdot\vec{A}$ contributions for high Z elements when $a/k < 1$.

2. General work and new additions

The DDCS (ejected electrons not observed) in IA is a product of a simple kinematical factor and the Compton profile $J(p_z)$, (units $\hbar = c = 1$ are used)

* Corresponding author. Address: R. Boskovic Institute, Bijenicka 54, 10000 Zagreb, Croatia. Tel.: +385 1 4680102; fax: +385 1 4680239.
E-mail address: suric@irb.hr (T. Suric).

0168-583X/$ - see front matter © 2007 Elsevier B.V. All rights reserved.
doi:10.1016/j.nimb.2007.03.085

$$\frac{d^2\sigma}{d\omega_f d\Omega_f} = \frac{1}{2}(1+\cos^2\theta)\frac{\omega_f}{\omega_i}\frac{m}{k}J(p_z), \quad (1)$$

where ω_i (ω_f) is incoming (outgoing) photon energy, $\vec{k}$ is the photon momentum transfer ($\vec{k} = \vec{k}_i - \vec{k}_f$) and θ is the photon scattering angle

$$J(p_z) = \int_{p_y}^{\infty} \rho(p) p dp, \text{ [e.g. for an H-like K-shell}$$

$$J(p_z) = \frac{8a^5}{3\pi(a^2+p^2)^3}, \quad a = mZ\alpha] \quad (2)$$

and $p_z = k/2 - m(\omega_i - \omega_f)/k$ is the component of the initial state electron momentum in the direction of the photon momentum transfer $\vec{k}$. The importance of the IA lies in this simple connection Eq. (1) between the observable (DDCS) and the structure [ρ(p)]. The IA predicts $J(p_z)$ is symmetric around $p_z = 0$. However, discrepancies have been found and are attributed to asymmetry around $p_z = 0$. We will discuss this issue, arguing that this is just a shift in the spectrum, while the asymmetry around the shifted peak position is very small.

A derivation of the IA from nonrelativistic A^2 approximation (which neglects the $\vec{p}\cdot\vec{A}$ term in the electron photon interaction) for the DDCS was given by Eisenberger and Platzman [2]. It was argued that with increasing incident photon energy (for which the $\vec{p}\cdot\vec{A}$ contribution can be neglected) the time scale on which the process occurs becomes short, which allows the cancellation of the electron final state potential energy with the electron initial state potential energy. In effect, this results in scattering of photons from a distribution of free electrons, which is just the IA. The IA was argued by EP to be justified in the Compton peak region if $(a^2/k^2)^2$ is small. However, for the DDCS the IA is commonly used, and viewed as adequate, in much more general circumstances, only requiring that $a/k < 1$.

While the IA utilizes the nonrelativistic photon–electron scattering, there is a corresponding relativistic version (RIA) introduced by Ribberfors [3]. In the RIA the DDCS is not just proportional to the Compton profile, $J(p_z)$. However, further approximations make it possible to write

$$\frac{d^2\sigma}{d\omega_f d\Omega_f} = \text{K.F.} \times (J(p_{min}) + C(J(p_{min}))), \quad (3)$$

where $C(J(p_{min}))$ is a correction which is very small at large angles, K.F. is now a relatively complex kinematical factor and p_{min} (which in [3] is given only approximately) is now given by $p_{min} = \sqrt{E_{min}^2 - m^2}$, where

$$E_{min} = \left[\frac{1}{4}(\omega_i - \omega_f)^2 + \frac{1}{2}\omega_i\omega_f(1-\cos\theta) + m^2\left(1 + \frac{(\omega_i-\omega_f)^2}{2\omega_i\omega_f(1-\cos\theta)}\right)\right]^{\frac{1}{2}} - \frac{1}{2}(\omega_i - \omega_f). \quad (4)$$

Here p_{min} (approximates p_z as defined in [3]) is a component of the initial state electron momentum in the direction of photon momentum transfer $\vec{k}$, now determined by relativistic kinematics.

Although the RIA employs the full electron–photon interaction, it cannot describe all aspects of the Compton spectrum (such as resonances and infrared divergences) since electrons are assumed free. The full relativistic independent particle approximation (IPA) S-matrix calculations of Compton scattering were performed in the early 1990s [4,5]. The S-matrix calculations use the full relativistic photon electron interaction (in second order) in a self consistent (IPA) potential. The numerical evaluation is performed with multipole and partial wave expansions, which make it necessary to perform numerically only radial matrix elements. The S-matrix calculations allow discussion of all three features of the Compton spectrum: the infrared divergent region (as $\omega_f \to 0$), the resonant region (for scattering with the ejection of an electron from a shell above the K-shell), and the Compton peak region (which is the only region treated by the IA or the RIA). The S-matrix approach also allows testing the validity of the much simpler RIA, and confirms its usefulness at relativistic energies except for K-shells of high Z atoms. While the RIA is valid for the DDCS for $a/k < 1$ for low Z elements (as in the nonrelativistic case), for high Z elements there are important contributions (neglected in the RIA) which correspond to the nonrelativistic $\vec{p}\cdot\vec{A}$ interaction. We find them important in the peak region only for scattering from high Z K-shells.

It should be pointed out that for the whole atom DDCS in the Compton peak region, the contributions of inner shells are much smaller than the contributions of outer shells (due to the number of electrons and due to the fact that at the peak the contribution of each bound electron is approximately inversely proportional to its average momentum, which is smaller for higher shells). For an inner shell electron the peak region is much broadened, with the same area. For the TDCS (when the angle of the outgoing electron is observed as well) the IA is also a well defined approach (despite an apparent violation of the conservation of energy), but its validity is only achieved for $a/k \ll 1$ [6].

3. Difference of TDCS and DDCS

The difference between the TDCS and the DDCS may be analyzed by looking at the analytical expressions for Coulombic K-shell matrix elements squared in the IA and in full A^2 approaches. These expressions differ in a simple angular dependent factor

$$\frac{(\vec{k}\cdot(\vec{k}-\vec{p}))^2 + \left(\frac{a}{p}(\vec{k}\cdot\vec{p})\right)^2}{(k^2-p^2+a^2)^2 + 4p^2a^2}, \quad (5)$$

where $\vec{p}$ is the outgoing electron momentum. While the IA for the DDCS is apparently valid for $a/k < 1$, for the TDCS its validity is achieved only for $a/k \ll 1$. This is illustrated in Fig. 1, where the DDCS (panel a) and the TDCS (panel b) are shown for the scattering of 59 keV photons from the

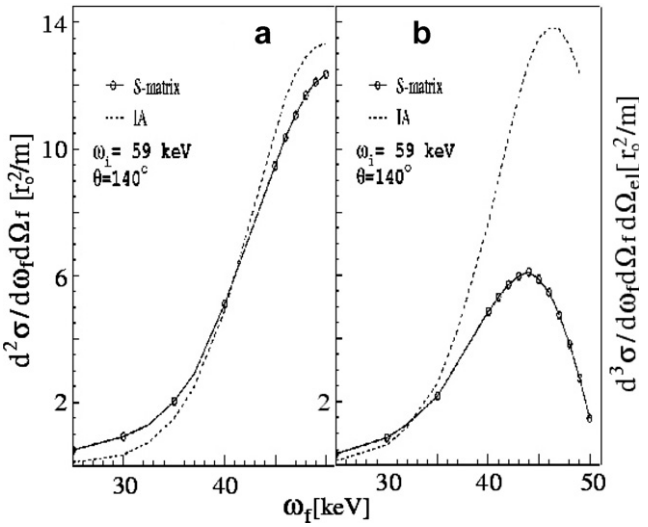

Fig. 1. DDCS (a) and TDCS (b) for the scattering of 59 keV photons from the K-shell of Cu into $\theta = 140°$ ($r_0 = \alpha/m$). In panel (b) electron momentum $\vec{p}$ is in the direction of momentum transfer $\vec{k}$.

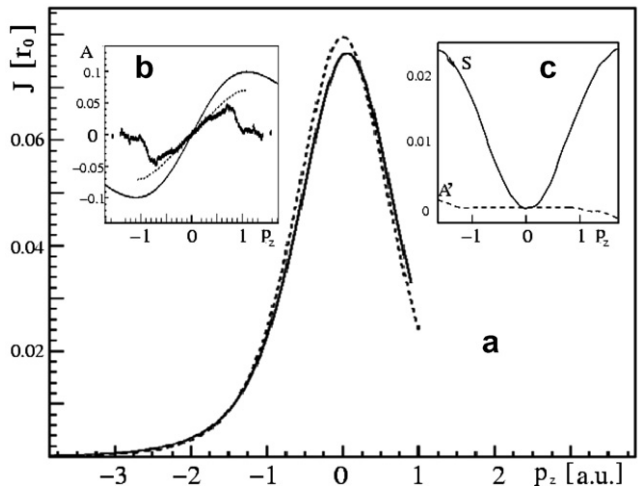

Fig. 2. (a) Coulombic (full line) and IA predictions (dotted line) of the Compton profile for the scattering of 10 keV photons from the K-shell of beryllium, for the scattering angle $\theta = 165°$, (b) asymmetry A, experimental data [8], Coulombic results (using Z_{eff}, solid line) and S-matrix results (dashes) are shown and (c) symmetric S and antisymmetric A' parts.

K-shell of Cu into $\theta = 140°$. The results are obtained by S-matrix calculations (from [7]) and by using the IA. Although $a/k \approx 1$, we see that DDCS is well described by the IA. The TDCS shown in panel b is calculated for electron momentum $\vec{p}$ in the direction of $\vec{k}$. However, the IA overestimates the TDCS by more than a factor of two. For other electron angles the IA underestimates the TDCS, and the average over all electron angles yields a good result for the DDCS. The validity of the IA is achieved for the electron spectrum (integrated over scattered photon angles) only when $a/k \ll 1$.

4. Asymmetry

The Compton profile deviates from IA predictions. This deviation is illustrated in Fig. 2 for the scattering of 10 keV photons from the K-shell of beryllium, for the scattering angle $\theta = 165°$. We have chosen an effective charge $Z_{\text{eff}} = 2.86$ to have a realistic binding energy and a profile for the K-shell of the Be atom. For this situation $a/k = 0.54$. The figure (panel a) shows Coulombic (with Z_{eff}) predictions (full line) and IA predictions (dotted line). One can see that the positions of the peaks in the two approaches differ by some amount $\delta(a/k)$, with the position of the peak of J^{IA} at $p_z = 0$. The heights of the peaks $J(\delta)$ and $J^{\text{IA}}(0)$ are also different, and $N(a/k)$ denotes their ratio. Since experiments usually measure only relative cross-sections, the experimental data are often normalized to theoretical values, and the remaining difference between IA predictions and measured values is expressed in terms of the so-called asymmetry

$$A(p_z) = \frac{J(p_z,k) - J(-p_z,k)}{J(0,k)}. \tag{6}$$

A slight inconsistency between the usual form of theoretical predictions and the usual experimental results should be noted before proceeding further. The variables which describe J can be taken as (p_z, k) or as (ω_f, θ), or otherwise. The theory often assumes that k is fixed and that p_z varies, as depicted in Fig. 2(a). However, experimentally θ is normally fixed and variation in ω_f is observed. When a/k is small, k is nearly constant in the peak region, so that variation in ω_f corresponds to variation in p_z. This has not been studied in more detail, as noted in [8].

An example of asymmetry data obtained for the beryllium atom (whole atom scattering) by Huotari et al. [8], for the scattering of 10 keV photons into $\theta = 165°$, is shown in Fig. 2(b), together with our K-shell Z_{eff} and S-matrix predictions with a screened potential. (Huotari et al. found experimentally that contributions from valence electrons to the asymmetry $A(p_z)$ are negligible.) Note that the overall magnitude and behavior are much better represented by S-matrix calculations. (Calculations of asymmetry in screened potential but within the A^2 approximation were performed for He and Ne by Wong et al. [9].)

It is evident that the deviation from the IA at these energies can be analyzed within an IPA picture. We have recently observed that asymmetry $A(p_z)$ is to a large extent just a shift of the spectrum (i.e. there is little asymmetry around the true peak, which is shifted by an amount δ from the IA peak at $p_z = 0$). We have found this result also for low Z elements in using our S-matrix code at relativistic energies. Hence, we suggest a new definition of asymmetry. The relative difference between a shifted Compton profile J (shifted by δ so that its maximum is at $p_z = 0$) and the IA prediction J^{IA} normalized by N to give the same peak value as J can be partitioned into small symmetric S and antisymmetric A' parts

$$\frac{J(p_z+\delta,k) - NJ^{\text{IA}}(-p_z)}{J(\delta,k)} = S(p_z,k) + A'(p_z,k). \tag{7}$$

The A' defined in this way is the true asymmetry of the Compton profile, while S is the main deviation from the IA shape. In Fig. 2(c), we show S and A' for the case of Fig. 2(a) and (c) shows that both S and A' are small, A' being about 0.1% at the largest p_z at which the experiment (Fig. 2(b)) was performed, and S being about 2%.

5. High Z behavior

We find the revised description of deviations from the IA in terms of (δ,N) also applicable at relativistic energies, except however for high Z K-shell Compton scattering. The difference in this case can be understood as due to the contribution of the $\vec{p}\cdot\vec{A}$ interaction term (neglected in the RIA) in the peak region for $a/k \approx 1$. We have performed an analysis (including for high Z) using our relativistic S-matrix numerical approach. We have indeed found that the $\vec{p}\cdot\vec{A}$ contribution to the peak region for $a/k \approx 1$ is important, but only for the scattering from high Z K-shells. For low Z elements, the contribution of the $\vec{p}\cdot\vec{A}$ term for $a/k \approx 1$ (or the relativistic analog of the $\vec{p}\cdot\vec{A}$ term) is negligible (as demonstrated below) and the RIA is found adequate under the same conditions as the IA.

The high Z behavior of the Compton profile is illustrated in Fig. 3 for the scattering of 450 keV photons from K-shell of uranium ($Z = 92$) into 90° (panel a) and 180° (b). The profiles are obtained using Eq. (3). The figure shows that the infrared behavior (rise of the profile as p_z becomes increasingly negative, which corresponds to $\omega_f \to 0$) for high Z is not separated from the peak region, which illustrates the importance of the $\vec{p}\cdot\vec{A}$ term when $a/k \approx 1$. (If we increase photon momentum transfer k so that $a/k \ll 1$, we obtain a situation similar to low Z cases for $a/k \approx 1$, i.e. the $\vec{p}\cdot\vec{A}$ contribution in the peak region decreases.)

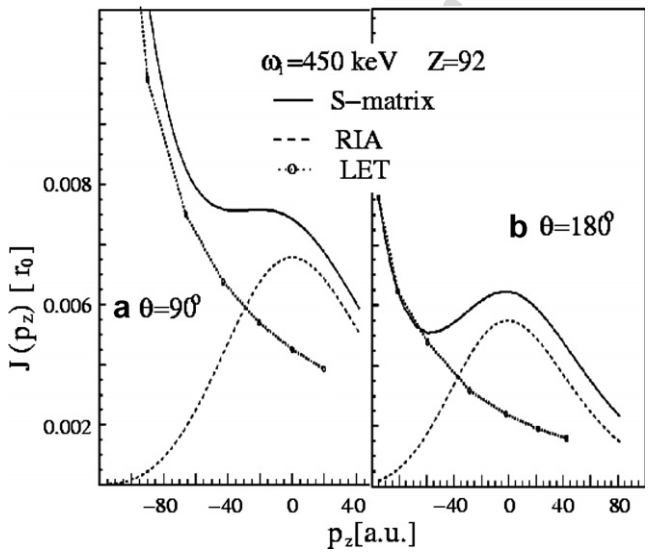

Fig. 3. The Compton profile for the scattering of 450 keV photons from K-shell of uranium ($Z = 92$) into 90° (a) and 180° (b).

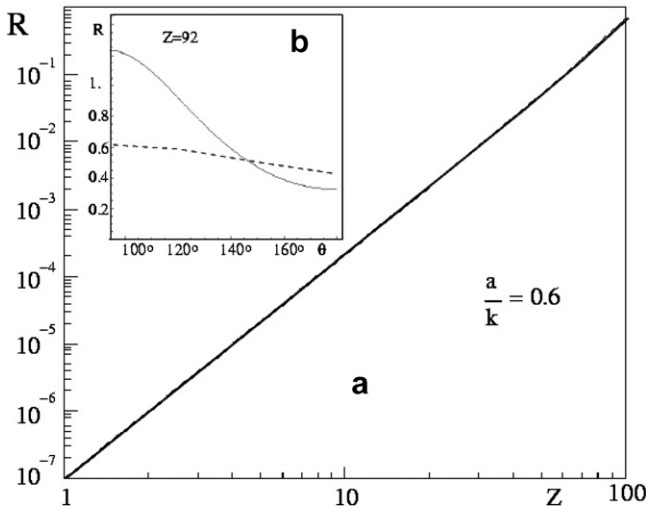

Fig. 4. (a) The ratio R is a function of Z for fixed $a/k = 0.6$ and (b) R is a function of angle for the case in Fig. 3.

In the limit $\omega_f \to 0$ the DDCS can be described in terms of photoeffect, by using the low-energy theorem [5]. (The low-energy theorem (LET) connects a radiative process (Compton) with the corresponding nonradiative process (photoeffect) in the $\omega_f \to 0$ limit.) Roughly, the DDCS is $\propto(1/\omega_f)/\sigma^{\text{photo}}$ and it is determined by the $\vec{p}\cdot\vec{A}$ term. The LET result is shown in Fig. 3 by dotted lines, which are extrapolated (by using the $1/\omega_f$ dependence) toward the peak region, in order to give at least a rough estimate of the $\vec{p}\cdot\vec{A}$ contribution in the peak region. R denotes the ratio between the LET result at the Compton peak and the RIA result at the Compton peak, and it gives us an estimate of the relative importance of the $\vec{p}\cdot\vec{A}$ term at the peak. We have analyzed Rboth by using S-matrix calculations and by using approximate analytic expressions for photoeffect to obtain the LET prediction. The results are shown in Fig. 4. Panel a shows R (obtained using approximate analytical expressions for the LET contribution) as a function of Z for fixed $a/k = 0.6$ (corresponding roughly to the case in Fig. 3). The figure exhibits a strong Z dependence (approximately Z^3 in our crude model) in R which gives that $\vec{p}\cdot\vec{A}$ contribution is important only for the K-shell of high Z atoms. Fig. 4(b) gives R as a function of angle for the case in Fig. 3 and shows estimates obtained both with the crude analytic formula and by extrapolating S-matrix calculations. We can see that these two rough estimates are of similar magnitude.

6. Summary

We have discussed the validity of impulse approximation, with particular attention to the kinematical region in which $a/k < 1$. In a nonrelativistic regime the IA for the DDCS is fairly good as long as $a/k < 1$, which is less restrictive than required by Eisenberger and Platzman. The same is true for the RIA at relativistic energies for low Z atoms. We have argued that the main discrepancies

between IA results for Compton profiles and the more exact results (which are usually called asymmetries) are in fact shifts of the profile, and we have found that the true asymmetry of the profile is very small. We have discussed the contribution of the $\vec{p}\cdot\vec{A}$ interaction term (neglected in the IA) in the peak region for $a/k \approx 1$. We have found that this contribution to the peak region is important for scattering from high Z K-shells.

Acknowledgements

This work has been supported by MZOS Grant No. 0098012 and by NSF Grant Nos. 0456499 and 0352483.

References

[1] Jesse W.M. Du Mond, Phys. Rev. 33 (1929) 643.
[2] P. Eisenberger, P.M. Platzman, Phys. Rev. A 2 (1970) 415.
[3] R. Ribberfors, Phys. Rev. B 12 (1975) 2067.
[4] T. Suric et al., Phys. Rev. Lett. 67 (1991) 189.
[5] P.M. Bergstrom et al., Phys. Rev. A 48 (1993) 1134.
[6] Z . Kaliman et al., Phys. Rev. A 57 (1998) 2683.
[7] Z. Kaliman et al., Fiz. A (Zagreb) 9 (2000) 1.
[8] S. Huotari et al., J. Phys. Chem. Solids 62 (2002) 2205.
[9] T.C. Wong et al., Phys. Rev. A 26 (1982) 181.